Eidgenössische Technische Hochschule Zürich
Swiss Federal Institute of Technology Zurich

Communication Technology Laboratory
Institut für Kommunikationstechnik

UWB Channel Modeling

Semester Thesis

Georg Böcherer

July 5, 2006

Professor: H. Bölcskei
Supervisor : Ulrich Schuster
Supervisor : Markus Gärtner

Acknowledgment

Ich möchte Ulrich Schuster danken für die vielen anregenden Diskussionen während des Semesters. Professor Helmut Bölcskei und seiner Gruppe möchte ich dafür danken, dass ich ein Semester lang in ihrem Institut arbeiten konnte.

Ich danke Wenji und Musa für ihre Gesellschaft und Unterstützung.

Meiner Mutter wünsche ich alles Gute für die kommende Zeit.

Zürich, den 5. Juli 2006

Georg Böcherer

Abstract

UWB channels are in general modeled as frequency selective fading channels. To be able to establish communication over such a channel, the current channel realization has to be estimated. In a base–band equivalent discrete time channel model, the unknown parameters would be the gain, the phase and the delay of the channel taps.

By using band-limited input signals, we can base the discrete time channel model on samples taken at the sender and the receiver. The estimation of the delay of the channel taps we can in this case reduce to the estimation of the timing offset between sender and receiver.

In this paper, we will show that modeling the timing offset can be omitted without loss of performance when modeling UWB channels. We show this for a general class of channel realizations which we define by reasonable assumptions for the physical channel.

Our results show that the commonly used base-band equivalent discrete time channel models which include in their stochastic characterization phase and gain of a finite number of taps only are in UWB communication robust against unknown timing offsets between sender and receiver in the sense that sampling clocks at sender and receiver do not need to be synchronized.

Contents

List of Figures

1. Introduction

In the last years, wireless communication over short distances has drawn a lot of attention. More and more people want to easily exchange multimedia data such as photos, music and video between cellular phones, handhelds and laptops. The data size is increasing, this leads to a strong demand for higher data rates.

Communication over channels with ultrawide bandwidth promises such very high data rates over short distances and a strong link reliability because of an increased frequency diversity.

Researchers have therefore started to investigate communication theoretic and information theoretic aspects of ultrawideband (UWB) channels. The first step in doing so is to model the UWB channel. Describing the reality by a model is a trade-off: a model can describe reality in a poor way but be analytically tractable. Similar, a model can describe a specific situation perfectly but does not characterize well the general case. The same problems occur in UWB channel modeling. Here, we will focus on modeling the UWB channel of an indoor environment in a typical public building.

So far, there have been several approaches to model the indoor UWB channel. They have in common the idea of multipath fading, which is a property frequently encountered in wireless channels [1]. Many authors construct their models in the following way: they interpret the physical channel as a superposition of a finite number of physical paths. Such a physical path could in reality be a sequence of several propagation mechanisms. An example would be: decoupling of a signal from the send antenna, reflection on a wall followed, reflection on a table and finally excitation of the receive antenna. The authors using this approach then try to map these physical paths to terms in their models. Examples for this approach you can find in [2] or [3]. The authors in [4] choose a different approach: they first assume the channel to be linear time invariant (LTI). This can be justified in the following way: in UWB communication, we have very large bandwidths. This results in a temporal resolution which is high compared to the slowly varying indoor environment. We can thus assume block fading [1] and we can assume the channel realization for every block to be LTI. The authors then argue in the following way: since the effective channel including signal processing at sender and receiver is band limited, it can be represented by its samples. Because the latter approach allows more general assumptions about the channel and because it results in a analytically tractable model, it seems advantageous. The discrete time model given in [4] is

$$y[k] = \sum_{l=0}^{L-1} h[l]x[k-l] \tag{1}$$

where the $y[k]$s, the $h[l]$s and the $x[k]$s are the output samples, the channel taps and the input samples and where L is the finite number of considered channel taps. The authors of [4] then perform extensive measurements of the UWB channel in a typical indoor environment and they give their results with respect to (1). The definition of the model seems reasonable from a realistic point of view, however, there are two possible problems of (1) which are not discussed in [4]:

- The fact that only a finite number of channel taps is considered would theoretically lead to a loss of information. According to the Sampling Theorem, a general band-limited signal can only be represented by a countable but infinite number of samples.
- The synchronization of the sampling processes at sender and receiver might have a significant influence onto how good the (discrete) model represents the (continuous) effective channel.

In the following chapters, we will investigate fundamental properties of band-limited signals in time domain to show that the following statements hold for UWB channels:

- Because of the large bandwidth, the effective impulse response of UWB channels can be sufficiently described by a finite number of channel taps.
- Because of the large bandwidth, the sampling processes at sender and receiver do not need to be synchronized in a small scale order.

These results encourage the usage of (1) to describe general indoor UWB channels.

Notation

A frequently used function is the sinc function which we define by

$$\operatorname{sinc}(t) = \begin{cases} \frac{\sin(\pi t)}{\pi t}, & t \neq 0 \\ 1, & t = 0. \end{cases} \tag{2}$$

Note that the sinc function defined in this way is continuous. The Fourier transform of a function $x(t)$ we denote by $X(f)$. In the same way, we denote the inverse Fourier transform of a function $X(f)$ by $x(t)$. We define the Fourier transform by

$$X(f) = \int_{-\infty}^{\infty} x(t) e^{-j2\pi f t}\, \mathrm{d}t. \tag{3}$$

We say that a function $x(t)$ is of bandwidth W if its Fourier transform fulfills $X(f) = 0$ whenever $|f| > W$. We say that a function $X(f)$ is of bandwidth W if $X(f) = 0$ whenever $|f| > W$. Additional notation we introduce throughout this paper when needed.

2. UWB Channel Model

The goal of this project is to propose a model to describe indoor UWB channels. We will proceed in the following way: We start by defining the term channel in the present context. We will then state some assumptions about the channel according to the specific scenario of an indoor environment. To arrive at a mathematical tractable description, we will then strictly band-limit the considered signals and define a discrete time model by applying the Sampling Theorem. This discrete time model we will truncate in time. We will show that this truncated discrete time model still is a good representation of the UWB channel because of the large bandwidths used in UWB communications.

Some mathematical derivations we postpone to the following chapter. Whenever we speak of signals in the following, we mean waveforms of finite energy as defined in [5].

2.1. Definition of the Channel

In communications, a frequently used term is the notion of a channel. A look at [6] illustrates that there is no strict definition of the term channel. However, we want to model an UWB channel so we have first to define what we actually mean by a channel. Thinking of a channel as the effects a physical environment has onto the electromagnetic signals between the antennas at sender and receiver is problematic. For different antenna parameters and different signals, the same physical environment can have completely different effects onto the signal, so it is impossible to find a complete description of a channel in this sense. In addition, even for a single pair of antennas and a specific signal, we will never see what the effects of the physical environment actually are. The only way to "see" electromagnetic waves is to measure them, but to measure them, we need antennas, so the measurements will show the effects of the physical environment and the antennas we used to measure the signals. To be precise, also this is a simplified view. After passing through the antenna, the signal will be processed through several electrical devices with capacities, resistances and inductances all having additional effects on the signals we finally see.

We will not deal with concrete implementation issues in this paper, but having this problematic in mind, we restrict our considerations to digital communication systems and assume that somewhere both in the sender and the receiver, the analogue signal is present in the baseband form. This could be for example right before sampling [7]. We include passband communication and combine the in-phase and quadrature components [8] of the signal; our analogue baseband signal might thus take complex values.

Throughout the rest of this paper, we will refer to the complex baseband signal at the sender by $x(t)$ and we will refer to the complex baseband signal at the receiver by $y(t)$. We define the channel as the operator H that maps $x(t)$ to $y(t)$. In the following, we will state some assumptions about H which allow us to describe H in a closed form.

2.2. Assumptions About the Channel

Linearity

It is convenient [1] to assume H to be linear in $x(t)$ (For now we will neglect components of $y(t)$ independent from $x(t)$. We could later add them in the form of additive noise). Although in practice H might be nonlinear for example because of nonlinear electrical devices at sender and receiver, we will assume H to be linear. We can thus describe H by a linear time varying system represented by a time varying impulse response $h(t, \tau)$. The mapping from $x(t)$ to $y(t)$ is then given by convolving $x(t)$ with $h(t, \tau)$:

$$y(t) = \int_{-\infty}^{\infty} h(t-\tau, \tau) x(\tau) \, \mathrm{d}\tau. \tag{4}$$

Time Invariance

We want to model the channel of typical indoor environments together with potential applications of UWB communication systems such as data links between laptops. In this scenario, the physical environment will variate slowly with respect to the high time resolution of an UWB signal. The stochastic characterization of H will therefore be of the block-fading type [1]. Consequently, we assume the parameters of H to be constant over one block and to change to an independent realization for the next block.

For every block, H is therefore time invariant and we can represent the mapping from $x(t)$ to $y(t)$ by convolving $x(t)$ with a time invariant impulse response $h(\tau)$:

$$y(t) = \int_{-\infty}^{\infty} h(t-\tau)x(\tau)\,\mathrm{d}\tau. \tag{5}$$

For the rest of this paper, we we will use $h(\tau)$ from (5) to represent H.

Finite Duration of $h(\tau)$

We assume that $h(\tau)$ takes nonzero values over a finite interval of length D_s in time. In literature, the parameter D_s is often called the delay spread of the channel [1]. We justify this assumption by physical reasoning: exciting the channel by a signal of finite duration at the sender will have perceivable effects at the receiver over a time interval of finite duration only.

2.3. Discrete Time Model

Band-Limited Input/Output Signals

As stated above, we can only measure $x(t)$ and $y(t)$ but not $h(\tau)$ in practice. One possible technique to find $h(\tau)$ anyhow is data aided (DA) estimation [9]: we measure the output $y(t)$ of the system for a known input $x(t)$ and then determine $h(\tau)$ from $x(t)$ and $y(t)$. We will base our further derivations on the idea of DA estimation. From a realistic point of view, we would like to consider a band-limited input signal of finite duration in time. Theoretically, this is unfortunately impossible. A strictly band-limited signal takes nonzero values over the whole time axis. In [10] you can find a discussion of this dilemma. We choose the following approach to deal with this problem: we assume that the input signal $x(t)$ takes nonzero values during a time interval of length D_x and we assume further, that the energy of $x(t)$ is in frequency domain concentrated in the interval $[-W, W]$. We then define $\tilde{x}(t)$ as $x(t)$ low-pass filtered by W. We can interpret $\tilde{x}(t)$ as $x(t)$ truncated in frequency domain. If the energy of the input signal $x(t)$ is concentrated in $[-W, W]$ then so is the energy of $h(t)$ and $y(t)$. This is a property of LTI systems: the convolution in time domain (5) corresponds to a multiplication of the frequency spectrums of $h(\tau)$ and $y(t)$ in frequency domain. We therefore define $\tilde{h}(t)$ and $\tilde{y}(t)$ as $h(t)$ and $y(t)$ low-pass filtered by W. The I/O relation (5) truncated in frequency domain becomes

$$\tilde{y}(t) = \int_{-\infty}^{\infty} \tilde{h}(t-\tau)\tilde{x}(\tau)\,\mathrm{d}\tau. \tag{6}$$

We interpret (6) as a good approximation of (5) and we will base or further derivations on (6).

Sampling the Truncated I/O Relation

We apply the Sampling Theorem as stated in [5]. It says that we can represent a signal band-limited to W by its samples taken at uniform intervals of length $T = 1/2W$. This applies to $\tilde{x}(t)$, $\tilde{h}(t)$ and $\tilde{y}(t)$. Sampling $\tilde{x}(t)$ can be done straight forward, but with respect to sampling $\tilde{y}(t)$, we rise the following question:

> What should we use as time reference at the receiver?

At first sight, we might take the time reference at the sender t also as the time reference at the receiver t_r. However, it takes some time for the signal to cover the distance a between sender and receiver, so this definition is questionable. We then might propose to define t_r as $t_s + a/c$ where c is the speed of light. But also this definition has a problem: What is the distance between sender and receiver when there is no line of sight (LOS) between sender and receiver? In communications, this problem is treated by time synchronization [9]. We will later discuss the synchronization problem in UWB in more depth; for now, we will choose an arbitrary time reference at the receiver given by $t_r = t - d$ with $d \in \mathcal{R}$ constant. In the following, we will refer to these time references by t and $t - d$. Thinking of a DA estimation at the receiver, we sample $\tilde{y}(t)$ with respect to the timing reference at the receiver. Since $\tilde{x}(t)$ and thereby its samples are known a priori, the timing reference at the receiver has no influence onto the samples of $\tilde{x}(t)$. We have for the samples

$$y[k] = \tilde{y}(kT + d), \quad k \in \mathcal{Z} \tag{7}$$

and

$$x[k] = \tilde{x}(kT), \quad k \in \mathcal{Z}. \tag{8}$$

We can relate $y[k]$ to $x[k]$ by a discrete convolution:

$$y[k] = \sum_{l=-\infty}^{\infty} h[l]x[k-l]. \tag{9}$$

Since the $x[k]$s and the $y[k]$s are known at the receiver, we can determine the $h[k]$s by solving the set of linear equations (9).

Note that for different d, the $y[k]$s and consequently the $h[k]$s might take different values. However, because of the Sampling Theorem and Lemma 5, we obtain for any $d \in \mathcal{R}$ an I/O relation of the form (9) equivalent to (6).

2.4. Truncation of the Discrete Time Model

We low-pass filtered the signals in (5) to get (6) because we wanted to base the further derivations on mathematical reasoning. The I/O relation (5) is still related to reality, it only represents it in a more tractable form. Our further proceeding should therefore also be related to reality. The discrete time model (9) however has a fundamental problem: first, we consider a countable but infinite number of samples, and second, we take samples over a time interval of infinite length. In reality, this is impossible. We therefore will restrict our consideration to a finite number of subsequent samples in the following and thus truncate (9) in time.

Truncating (9) in time has two problematic consequences:

1. We have to decide which samples of $\tilde{y}(t)$ we take into account.
2. Although Lemma 5 shows that (9) is equivalent to (6) for any $d \in \mathcal{R}$, the quality of the discrete I/O relation truncated in time depends on d in general.

The quality of the truncated sample sequence we define by how good it represents $\tilde{h}(\tau)$. From the truncated sample sequence, we can construct an approximation of $\tilde{h}(\tau)$ by interpolating the sequence with sinc functions. This approximation is equal to $\tilde{h}(\tau)$ in every sample of the truncated sequence. According to Lemma 6 and Lemma 7 the energy of a band-limited signal is equal to the energy of its sampling sequence. We can therefore measure how good the approximation is in points different from the samples of the truncated sequence by comparing the energy of $\tilde{h}(\tau)$ with the energy of the truncated sequence: if the energy of the truncated sequence is equal to the energy of $\tilde{h}(\tau)$, then the truncated sequence perfectly represents $\tilde{h}(\tau)$. We will therefore use as a measure of the quality of the truncated sequence its energy compared to the energy of $\tilde{h}(\tau)$.

Note that comparing to functions by their energy is in general not a good measure in a point-wise sense.

Choice of Input Signal

We want to treat the two problems stated above fundamentally and not for a specific set of input/output signals $x(t)$ and $y(t)$. To find an optimal input signals $x(t)$ in DA estimation is a challenging task; we will not deal with this here.

We choose the following approach: we assume for the input samples

$$x[k] = \delta[k]. \tag{10}$$

This is consistent with our upper derivations since $x[k] = \delta[k]$ can be interpreted as the result of sampling

$$\tilde{x}(t) = \operatorname{sinc}\left(\frac{t}{T}\right) \tag{11}$$

which is band limited to $W = 1/2T$. For $y[k]$ we get

$$y[k] = \sum_{l=-\infty}^{\infty} h[l]x[k-l] \tag{12}$$

$$= h[k] \tag{13}$$

and we can restrict our considerations on how good a truncated sequence of samples $h[k] = \tilde{h}(kT + d)$ represents $\tilde{h}(\tau)$. We will denote this truncated sequence of subsequent samples of $\tilde{h}(\tau)$ by S.

Large Scale Synchronization

First we will formulate an approach how we deal with problem 1. We assumed $h(\tau)$ to take nonzero values over an interval of length D_s. We denote this interval by $[t_0, t_0 + D_s]$. We low-pass filtered $h(\tau)$ by W to get $\tilde{h}(\tau)$. As discussed in Appendix D, low-pass filtering with bandwidth W smoothes out local variations over intervals smaller then $T = 1/2W$ in time domain but preserves the large scale character of the signal. Since W is large in UWB communication, T will be small with respect to D_s. The filtered impulse response $\tilde{h}(\tau)$ will therefore have a form close to $h(\tau)$. The characteristic that $h(\tau)$ takes nonzero values over an interval of length D_s will not get completely lost; $\tilde{h}(\tau)$ still will have its main part of energy concentrated in the interval $[t_0, t_0 + D_s]$. We therefore assume that the receiver can determine an interval U of length $N > D_s$ which contains the interval $[t_0, t_0 + D_s]$. This could be achieved in the following way:

- The receiver determines the start of the interval U by a threshold rule.
- The length of the interval N is chosen to be a bit larger then an empiric value for typical delay spreads of UWB channels.

We call this assumption the large scale synchronization assumption.

Energy Bound for the Truncated Sample Sequence

We choose an arbitrary time reference $t + d$ at the receiver and consider the sequence S of samples in U. Without loss of generality, we assume $t_0 = 0$. In this case, we have $[0, D_s] \subset U$. It follows that the set of samples

$$\left\{\tilde{h}(lT + d')\right\}_{l=0}^{\lfloor D_s/T \rfloor - 1}, \quad d' \in \left[-\frac{T}{2}, \frac{T}{2}\right] \tag{14}$$

is among the samples in S. We can therefore bound the energy of the samples considered at the receiver by

$$\|h\|^2 \leq \|\tilde{h}\|^2 \geq \|S\|^2 \geq \sum_{l=0}^{\lfloor D_s/T \rfloor - 1} T \left|\tilde{h}(lT + d')\right|^2. \tag{15}$$

the term on the right side follows from the general discrete time base-band equivalent of signals. You can find an extensive derivation in Appendix C.

In UWB communication, we are interest in the system behavior for large $W = 1/2T$. In Appendix A we show that

$$\lim_{T \to 0} \sum_{l=0}^{\lfloor D_s/T \rfloor - 1} T \left|\tilde{h}(lT + d')\right|^2 = \|h\|^2. \tag{16}$$

For large W, S is therefore a very good representation of $\tilde{h}$.

2.5. UWB Channel Model

We have shown that choosing an arbitrary time reference at the receiver and using a simple synchronization rule (large scale synchronization assumption) leads to a finite sequence of samples which is a good representation of $\tilde{h}(\tau)$ for large W. The introduction of $\tilde{x}(\tau)$, $\tilde{y}(\tau)$ and $\tilde{h}(\tau)$ however was only an auxiliary definition to allow strict mathematical reasoning. We therefore resort to the original input and output functions $x(t)$ and $y(t)$ and define as a discrete time channel model of indoor UWB channels the set of samples $h[l]$ such that

$$y[k] = \sum_{l=0}^{L-1} h[l]x[k-l] \tag{17}$$

where the $y[k]$s and the $x[k]$s are samples of $x(t)$ and $y(t)$. This model gives a good characterization of the indoor UWB channel for L being large ($L > D_s/T$ for $W = 1/2T$ large) under the condition that the large scale synchronization assumption is fulfilled.

3. Conclusion

The main result of this project is that the discrete time input-output relation

$$y[k] = \sum_{l=0}^{L-1} h[l]x[k-l] \tag{18}$$

as defined in [4] is a good choice to represent a general indoor UWB channel. The time reference at the receiver can be chosen arbitrary and the only requirement is large scale synchronization, which is sometimes called time acquisition.

Our results have interesting consequences: other authors derived I/O relations similar to (18) from much more restrictive assumptions about the physical environment or they used heuristic argumentation. But since we could show that (18) is a good model for general indoor UWB channels, the results derived for (18) are fundamental and can be assumed to apply to general indoor UWB channels.

Together with the stochastic characterization of the channel taps based on extensive measurements given in [4], (18) seems to be a strong instrument for further investigations of the indoor UWB channel.

For UWB receiver design, our results indicate that synchronization issues should be rethought for UWB digital communications, since the high temporal resolution of UWB signals leads when sampling to large sets of samples describing the channel impulse response. Because of the properties of band-limited signals in time domain discussed in this paper, this relaxes requirements on small scale synchronization and allows sampling clocks at sender and receiver to be unsynchronized.

Further investigations of time synchronization in UWB communication might incorporate time variance of the channel and more general relations between the time references at sender and receiver. The time reference at sender would still be t and the time reference at the receiver would become $t - d(t)$. This way, also possible time drifts and frequency offsets of the sampling clocks at sender and receiver might be modeled.

A. Asymptotic Optimality

In Chapter 2, we ended up in our derivations with the following term:

$$\sum_{l=0}^{\lfloor D_s/T \rfloor - 1} T \left| \tilde{h}(lT + d) \right|^2, \quad d \in \left[-\frac{T}{2}, \frac{T}{2} \right]. \tag{19}$$

where we substituted d' by d to simplify notation. To avoid confusion, we will recall and make more precise the assumptions we made about $h(\tau)$ and $\tilde{h}(\tau)$. We will then prove that (19) goes to $\|h\|^2$ for $T = 1/2W$ going to zero.

A.1. Assumptions About the Channel

We assume that the unfiltered channel impulse response $h(\tau)$ has a delay spread D_s, which means that $h(\tau)$ is zero outside some interval of length D_s. Without loss of generality, we assume this interval to be $[0, D_s]$. In this interval, we assume that every realization $h(\tau)$ takes essentially finite values, we can thus bound $|h(\tau)|$ by some finite $h_{\max} \in \mathcal{R}$ defined as:

$$h_{\max} = \operatorname*{ess\,sup}_{\tau \in \mathcal{R}} h(\tau). \tag{20}$$

Note that $h_{\max}$ can be different for different realizations.

These assumptions imply an additional property of $h(\tau)$ which we will need later. We state this property as a proposition:

Proposition 1. *If we filter $h(\tau)$ by a continuous filter, the result is continuous.*

Proof

Let $f : \mathcal{R} \to \mathcal{R}$, $\tau \to f(\tau)$ be a function continuous in $\mathcal{R}$. To prove that $y(t) = (h \star f)(t)$ is continuous we have to show that for any $a \in \mathcal{R}$, the term

$$|y(t) - y(a)| \tag{21}$$

goes to 0 for $t \to a$. We have

$$|y(t) - y(a)| = \left| \int_{-\infty}^{\infty} f(t-\tau) h(\tau) \,\mathrm{d}\tau \int_{-\infty}^{\infty} f(a-\tau) h(\tau) \,\mathrm{d}\tau \right| \tag{22}$$

$$= \left| \int_{0}^{D_s} \left(f(t-\tau) - f(a-\tau) \right) h(\tau) \,\mathrm{d}\tau \right| \tag{23}$$

$$\leq \int_{0}^{D_s} \left| \left(f(t-\tau) - f(a-\tau) \right) h(\tau) \right| \,\mathrm{d}\tau \tag{24}$$

$$\leq h_{\max} \int_{0}^{D_s} \left| \left(f(t-\tau) - f(a-\tau) \right) \right| \,\mathrm{d}\tau. \tag{25}$$

We assume t to be close to a, we thus consider $f(\tau)$ in a compact interval and in this interval, $f(\tau)$ is uniformly continuous. We have

$$\forall \epsilon > 0 \; \exists \delta : \forall t, a : |t-a| < \delta : \tag{26}$$

$$|y(t) - y(a)| \leq h_{\max} \int_{t_0}^{t_0+D_s} |(f(t-\tau) - f(a-\tau))| \, \mathrm{d}\tau \tag{27}$$

$$\leq h_{\max} \int_{t_0}^{t_0+D_s} |\epsilon| \, \mathrm{d}\tau \tag{28}$$

$$= h_{\max} D_s \epsilon. \tag{29}$$

This proves the proposition.

□

A.2. Proposition and Proof

Proposition 2. *Let $\tilde{h}(\tau)$ be equal to $h(\tau)$ low-pass filtered by W, which implies for the frequency spectrum*

$$\tilde{H}(f) = H(f)\mathrm{rect}(f, W)\,. \tag{30}$$

Then for $T = 1/2W$ and $d \in [-T/2, T/2]$ the term

$$\sum_{l=0}^{\lfloor D_s/T \rfloor - 1} T \left| \tilde{h}(lT + d) \right|^2 \tag{31}$$

converges to $\|h\|^2$ for $T \to 0$.

Proof

To be able to prove the proposition, we need to consider the bandwidth W of $\tilde{h}(\tau)$, the sampling time T and the timing offset d separately. We will denote the sampling time by T_r. To the bandwidth W we will refer by $T = 1/2W$. The timing offset we will denote by d as before. Treating T_r, T and d separately means that when we change the value of one of these variables in the following, the other variables remain constant.

To simplify notation, we introduce the symbol $\|E\|^2$:

$$\|E\|^2 = \sum_{l=0}^{\lfloor D_s/T_r \rfloor - 1} T_r \left| \tilde{h}(lT_r + d) \right|^2 . \tag{32}$$

Since $\tilde{h}(\tau)$ is the result of filtering $h(\tau)$ by a continuous function (the inverse Fourier transform of $\mathrm{rect}(f, W)$ is a sinc function, which is continuous), it is according to proposition 1 continuous and the sum on the right half side (RHS) of (32) is for fixed d and T

the Riemann sum of $|\tilde{h}(\tau + d)|^2$ over the interval $[0, D_s]$. Letting T_r go to 0 we have

$$\lim_{T_r \to 0} \sum_{l=0}^{\lfloor \frac{D_s}{T_r} \rfloor - 1} T_r \left| \tilde{h}(lT_r + d) \right|^2 = \int_0^{D_s} \left| \tilde{h}(\tau + d) \right|^2 \mathrm{d}\tau. \tag{33}$$

According to Theorem 1 (Plancherel), $\tilde{h}(\tau)$ converges to $h(\tau)$ in the $\mathcal{L}^2(\mathcal{R})$ sense for $T \to 0$ (which means $W \to \infty$) and we get

$$\lim_{T \to 0} \int_0^{D_s} \left| \tilde{h}(\tau + d) \right|^2 \mathrm{d}\tau = \int_0^{D_s} |h(\tau + d)|^2 \mathrm{d}\tau. \tag{34}$$

Finally, we let d go to 0 and get

$$\lim_{d \to 0} \int_0^{D_s} |h(\tau + d)|^2 \mathrm{d}\tau = \int_0^{D_s} |h(\tau)|^2 \mathrm{d}\tau \tag{35}$$

$$= \|h\|^2, \tag{36}$$

so for $T_r \to 0$, $T \to 0$ and $d \to 0$ in this order, we have shown that $\|E\|^2$ goes to $\|h\|^2$ which is the desired result, since we cannot do any better ($\|E\|^2$ is a lower bound of $\|h\|^2$). Unfortunately, the convergence of this repeated limit does not imply the convergence of $\|E\|^2$ to the same value when we identify T_r with T, let d take values in $[-T_r/2, T_r/2]$ with $T_r = T$ and then consider the limit $T \to 0$. A discussion of the problem that repeated limits and double limits of the same term do not necessary converge to the same value you can find in standard textbooks on analysis.

However, we will prove in the following that $\|E\|^2$ goes to $\|h\|^2$ if we let (T_r, T, d) go to $(0, 0, 0)$ along any path with $T_r \leq T$. We will do this by approximating $\|h\|^2$ by $\|E\|^2$ by slightly decreasing the values of T, T_r and d.

First Approximation. From Theorem 1 (Plancherel) it follows that the integral

$$\int_{-\infty}^{\infty} \left| h(\tau) - \tilde{h}(\tau) \right|^2 \mathrm{d}\tau \tag{37}$$

goes to 0 for $T \to 0$. Since the support of $h(\tau)$ is $[0, D_s]$, also

$$\int_0^{D_s} \left| h(\tau) - \tilde{h}(\tau) \right|^2 \mathrm{d}\tau \tag{38}$$

goes to 0. For any $v, w \in \mathcal{L}^2(\mathcal{R})$, the reverse triangular inequality states that

$$|\|v\| - \|w\|| \leq \|v - w\| \tag{39}$$

and it follows that

$$\left| \int_0^{D_s} |h(\tau)|^2 \, \mathrm{d}\tau - \int_0^{D_s} \left|\tilde{h}(\tau)\right|^2 \, \mathrm{d}\tau \right| \tag{40}$$

also goes to 0 for $T \to 0$. But this is equivalent to

$$\forall \epsilon_1 > 0 \, \exists T_1 : \forall T < T_1 : (40) < \epsilon_1. \tag{41}$$

Second Approximation. Since $\tilde{h}(\tau)$ is continuous according to Proposition 1, it is uniformly continuous over compact intervals and the term

$$\left| \int_0^{D_s} \left|\tilde{h}(\tau)\right|^2 \, \mathrm{d}\tau - \int_0^{D_s} \left|\tilde{h}(\tau + d)\right|^2 \, \mathrm{d}\tau \right| \tag{42}$$

converges to 0 for $d \to 0$, which is equivalent to

$$\forall \epsilon_2 > 0 \, \exists T_2 : \forall \, |d| < \frac{T_2}{2} : (42) < \epsilon_2. \tag{43}$$

Third Approximation. Since $\tilde{h}(f)$ is continuous and since we consider it in a compact interval, the term

$$\left| \int_0^{D_s} \left|\tilde{h}(\tau + d)\right|^2 \, \mathrm{d}\tau - \sum_{l=0}^{\lfloor \frac{D_s}{T_r} \rfloor - 1} T_r \left|\tilde{h}(lT_r + d)\right|^2 \right| \tag{44}$$

converges to 0 for $T_r \to 0$ (Riemann sum). This is equivalent to

$$\forall \epsilon_3 > 0 \, \exists T_3 : \forall T_r < T_3 : (44) < \epsilon_3. \tag{45}$$

We define $\epsilon_0 = \epsilon_1 + \epsilon_2 + \epsilon_3$ and $T_0 = \min\{T_1, T_2, T_3\}$. Putting the 3 approximations together, we have shown that the term

$$\left| \int_0^{D_s} |h(\tau)|^2 \, \mathrm{d}\tau - \sum_{l=0}^{\lfloor \frac{D_s}{T_r} \rfloor - 1} T_r \left|\tilde{h}(lT_r + d)\right|^2 \right| = \left| \int_{-\infty}^{\infty} |h(\tau)|^2 \, \mathrm{d}\tau - \sum_{l=0}^{\lfloor \frac{D_s}{T_r} \rfloor - 1} T_r \left|\tilde{h}(lT_r + d)\right|^2 \right| \tag{46}$$

$$= \left| \|h\|^2 - \sum_{l=0}^{\lfloor \frac{D_s}{T_r} \rfloor - 1} T_r \left|\tilde{h}(lT_r + d)\right|^2 \right| \tag{47}$$

converges to 0 in the sense that

$$\forall \epsilon_0 > 0 \, \exists T_0 : \forall T, T_r, 2\,|d| < T_0 : (46) < \epsilon_0, \tag{48}$$

so (46) converges to 0 along the path indicated by the rule given in the proposition. This completes the proof.

□

Remark 1. *We proved the convergence along the special path $T_r = T$ and $d \in [-T_r/2, T_r/2]$, but the approximations 1–3 allow us to show the convergence for any path with $T_r \leq T$, so the convergence is also guaranteed when $T_r < T$, which corresponds to oversampling at the receiver.*

B. Mathematical Properties of Band-Limited Signals

In this chapter, we will define the Hilbert space of band-limited $\mathcal{L}^2(\mathcal{R})$ functions and show some useful properties of this space. We interpret $\mathcal{L}^2(\mathcal{R})$ as a vector space whose elements are equivalence classes formed by functions with a finite $\mathcal{L}^2(\mathcal{R})$ norm. The functions forming an equivalence class are equal almost everywhere with respect to the Lebesgue measure (a.e) of $\mathcal{R}$. However, we will follow the convention not to differ explicitly between equivalence classes and their representatives in notation.

Most of the material introduced in this chapter can be found in a similar form in [11]. For an introduction to Lebesgue integrals, measure theory and the $\mathcal{L}^p$ spaces I refer to [12].

Definition 1. *We define the Hilbert space $\mathcal{H}_W$ as the space of $\mathcal{L}^2(\mathcal{R})$ functions that are band-limited to W in the frequency domain:*

$$\mathcal{H}_W = \{V(f) \in \mathcal{L}^2(\mathcal{R}) | V(f) = 0 \qquad \text{whenever } |f| > W\}. \tag{49}$$

Remark 2. *Any $V(f) \in \mathcal{H}_W$ we can write as*

$$V(f) = V(f) \cdot \mathrm{rect}(f, W) \tag{50}$$

where $\mathrm{rect}(f, W)$ *denotes the unit gain low-pass filter of bandwidth W given by*

$$\mathrm{rect}(f, W) = \begin{cases} 1, & -W < |f| \leq W \\ 0, & \text{otherwise.} \end{cases} \tag{51}$$

Lemma 1. *The set of functions*

$$\Phi_l(f) = \frac{1}{\sqrt{2W}} e^{-j2\pi f l \frac{1}{2W}} \mathrm{rect}(f, W)\,, \quad l \in \mathcal{Z} \tag{52}$$

is a complete orthonormal basis of $\mathcal{H}_W$.

Proof

The truncated trigonometric Fourier series of $V(f)$ is given by

$$S_V^N(f) = \sum_{l=-N}^{N} \left\langle V(\nu), \tilde{\Phi}_l(\nu) \right\rangle \tilde{\Phi}_l(f) \tag{53}$$

with

$$\tilde{\Phi}_l(f) = \frac{1}{\sqrt{2W}} e^{-j2\pi f l \frac{1}{2W}}. \tag{54}$$

The Representation theorem (you can find it in any standard textbook in analysis) states that $\{\tilde{\Phi}_l(f)\}_{l\in\mathcal{Z}}$ is a complete orthonormal base of $\mathcal{H}_W|_{|f|\leq W}$ in the sense that

$$\lim_{N\to\infty}\int\limits_{-W}^{W}\left|V(f)-S_V^N(f)\right|^2\,\mathrm{d}f=0. \tag{55}$$

Since every $V(f)\in\mathcal{H}_W$ is equal zero outside the interval $[-W,W]$, we have

$$\begin{aligned}V(f)&=\sum_{l=-\infty}^{\infty}\left\langle V(\nu),\tilde{\Phi}_l(\nu)\right\rangle\tilde{\Phi}_l(f)\mathrm{rect}(f,W) &(56)\\ &=\sum_{l=-\infty}^{\infty}\left\langle V(\nu),\tilde{\Phi}_l(\nu)\mathrm{rect}(f,W)\right\rangle\tilde{\Phi}_l(f)\mathrm{rect}(f,W)\,. &(57)\end{aligned}$$

We define

$$\Phi_l(f)=\tilde{\Phi}_l(f)\mathrm{rect}(f,W) \tag{58}$$

and note that

$$\{\Phi_l(f)\}_{l\in\mathcal{Z}} \tag{59}$$

forms a complete orthonormal basis of $\mathcal{H}_W$.

□

Lemma 2. *Any phase-shifted version*

$$\Phi_l(f)=\frac{1}{\sqrt{2W}}e^{-j2\pi fl\frac{1}{2W}}\mathrm{rect}(f,W)\,e^{-j2\pi fd},\quad l\in\mathcal{Z},d\in\mathcal{R} \tag{60}$$

of (52) *is a complete orthonormal basis of* $\mathcal{H}_W$.

Proof

For an arbitrary $d\in\mathcal{R}$, we have for any function $V(f)\in\mathcal{H}_W$ another function $\tilde{V}(f)\in\mathcal{H}_W$ such that

$$V(f)=\tilde{V}(f)e^{-j2\pi fd}. \tag{61}$$

We now represent $V(f)$ by (59) and get

$$\begin{aligned} V(f) &= \tilde{V}(f)e^{-j2\pi fd} && (62)\\ &= e^{-j2\pi fd}\sum_{l=-\infty}^{\infty}\left\langle \tilde{V}(\nu),\Phi_l(\nu)\right\rangle \Phi_l(f) && (63)\\ &= \sum_{l=-\infty}^{\infty}\left\langle \tilde{V}(\nu),\Phi_l(\nu)\right\rangle \Phi_l(f)e^{-j2\pi fd} && (64)\\ &= \sum_{l=-\infty}^{\infty}\left\langle \tilde{V}(\nu)e^{-j2\pi fd},\Phi_l(\nu)e^{-j2\pi fd}\right\rangle \Phi_l(f)e^{-j2\pi fd} && (65)\\ &= \sum_{l=-\infty}^{\infty}\left\langle V(\nu),\Phi_l(\nu)e^{-j2\pi fd}\right\rangle \Phi_l(f)e^{-j2\pi fd}. && (66)\\ & && (67) \end{aligned}$$

Obviously, the set

$$\left\{\Phi_l(f)e^{-j2\pi fd}\right\}_{l\in\mathcal{Z}} \tag{68}$$

spans $\mathcal{H}_W$. It remains to show that the elements are orthonormal. We have

$$\begin{aligned} \left\langle \Phi_l(f)e^{-j2\pi fd},\Phi_k(f)e^{-j2\pi fd}\right\rangle &= \int_{-\infty}^{\infty}\Phi_l(f)e^{-j2\pi fd}\Phi_k^*(f)e^{j2\pi fd}\,\mathrm{d}f && (69)\\ &= \int_{-\infty}^{\infty}\Phi_l(f)\Phi_k^*(f)\,\mathrm{d}f && (70)\\ &= \left\langle \Phi_l(f),\Phi_k(f)\right\rangle, && (71) \end{aligned}$$

the orthonormality of (68) follows thus directly from the orthonormality of (59), and we conclude that (68) is an orthonormal basis of $\mathcal{H}_W$.

□

Lemma 3. *The Hilbert space $\mathcal{H}_W$ is invariant under any LTI tranformation with frequency spectrum $H(f)$ essentially (a.e.) taking finite values in $[-W,W]$.*

Proof

Let $X(f)\in\mathcal{H}_W$ be the frequency spectrum of the input function. The frequency spectrum of the output function of the LTI system is then given by

$$\begin{aligned} Y(f) &= X(f)H(f) && (72)\\ &= X(f)H(f)\mathrm{rect}(f,W) && (73) \end{aligned}$$

where the second line follows from the fact that $X(f)$ vanishes outside the interval $[-W,W]$ per definition. This implies that $Y(t)$ also vanishes outside the interval $[-W,W]$

and it remains to show that $Y(t) \in \mathcal{L}^2(\mathcal{R})$. We defined $H(f)$ to essentially take finite values in $[-W, W]$, we can thus upper bound the amount of $H(f)$ by some $c \in \mathcal{R}$:

$$|H(f)| \leq c \quad \text{a.e. for} f \in [-W, W]. \tag{74}$$

Using this we get for the squared 2-norm (the squared norm of $\mathcal{L}^2(\mathcal{R})$) of $Y(f)$:

$$\begin{aligned}
\|Y\|^2 &= \int_{-\infty}^{\infty} |Y(f)|^2 \,\mathrm{d}f && (75)\\
&= \int_{-\infty}^{\infty} |X(f)H(f)\mathrm{rect}(f, W)|^2 \,\mathrm{d}f && (76)\\
&= \int_{-\infty}^{\infty} |X(f)|^2 \,|H(f)\mathrm{rect}(f, W)|^2 \,\mathrm{d}f && (77)\\
&\leq \int_{-\infty}^{\infty} |X(f)|^2 \, c^2 \,\mathrm{d}f && (78)\\
&= c^2 \,\|X(f)\|^2 && (79)\\
&< \infty && (80)
\end{aligned}$$

and we can conclude that $Y(f) \in \mathcal{H}_W$. The Hilbert space $\mathcal{H}_W$ is thus invariant under LTI transformations whose frequency spectrum essentially take finite values in the interval $[-W, W]$.

□

Theorem 1. *(Plancherel) Let $\mathcal{S}$ be the set of rapdidly decreasing functions. Then*

1. *The restrictions $\mathrm{F}|\mathcal{S}$ and $\mathrm{F}^{-1}|\mathcal{S}$ of the Fourier transform F and its inverse F^{-1} on $\mathcal{S}$ can be uniquely extended to unitary operators $\mathcal{F}$ and $\mathcal{F}^{-1}$ on $\mathcal{L}^2(\mathcal{R})$.*

2. *$\mathcal{F}\,\phi = \mathrm{F}\phi$ and $\mathcal{F}^{-1}\,\phi = \mathrm{F}^{-1}\phi$ for any $\phi \in \mathcal{L}^2(\mathcal{R}) \cap \mathcal{L}^1(\mathcal{R})$.*

3. *For the extended Fourier transform for any $x(t) \in \mathcal{L}^2(\mathcal{R})$ it holds that*

$$\mathcal{F}\,x = \lim_{T_0 \to \infty} \int_{-T_0}^{T_0} x(t) e^{-j2\pi f t} \,\mathrm{d}t \tag{81}$$

and for the extended inverse Fourier transform for any $X(f) \in \mathcal{L}^2(\mathcal{R})$ it holds that

$$\mathcal{F}^{-1}\,X = \lim_{W \to \infty} \int_{-W}^{T_0} X(f) e^{j2\pi f t} \,\mathrm{d}f. \tag{82}$$

Remark 3. *Throughout this document, we think of $\mathcal{F}$ and $\mathcal{F}^{-1}$ when applying the Fourier transform and its inverse.*

Proof

A proof of the general case is given in [13]. Here we will only give a proof of property 3 in a special case.

Let $h(\tau) \in \mathcal{L}^2(\mathcal{R})$ be a function essentially taking nonzero values over the interval $[0, D_s]$. Let in addition the values in $[0, D_s]$ essentially be finite, such that we can bound $|h(\tau)|$ by some $h_{\max}$ defined in the following way:

$$h_{\max} = \operatorname*{ess\,sup}_{\tau\in\mathcal{R}} h(\tau). \tag{83}$$

Let $H(f)$ be the frequency spectrum of $h(\tau)$ and define $h_{\text{eff}}(\tau)$ as the inverse Fourier transform of

$$H_{\text{eff}}(f) = H(f)\text{rect}(f, W)\,. \tag{84}$$

For the squared 2-norm of $H_{\text{eff}}(f)$ we get:

$$\|H_{\text{eff}}\|^2 = \int_{-\infty}^{\infty} H_{\text{eff}}(f) H_{\text{eff}}^*(f)\,\mathrm{d}f \tag{85}$$

$$= \int_{-\infty}^{\infty} \left(H(f) - R_W(f)\right)\left(H(f) - R_W(f)\right)^2\,\mathrm{d}f \tag{86}$$

$$= \int_{-\infty}^{\infty} H(f)H^*(f)\,\mathrm{d}f - 2\Re\left\{\int_{-\infty}^{\infty} H(f)R_W^*(f)\,\mathrm{d}f\right\} + \int_{-\infty}^{\infty} R_W(f)R_W^*(f)\,\mathrm{d}f \tag{87}$$

$$= \|H\|^2 - 2\Re\left\{\int_{-\infty}^{\infty} H(f)R_W^*(f)\,\mathrm{d}f\right\} + \|R_W\|^2\,. \tag{88}$$

We can now upper- and lower-bound $\|H_{\text{eff}}\|^2$. An upper bound is given by

$$\|H_{\text{eff}}\|^2 \leq \|H\|^2 \tag{89}$$

and since $\|R_W\|^2 \geq 0$, a lower bound is given by

$$\|H_{\text{eff}}\|^2 \geq \|H\|^2 - \left|2\Re\left\{\int_{-\infty}^{\infty} H(f)R_W^*(f)\,\mathrm{d}f\right\}\right|. \tag{90}$$

To further bound the RHS of (90), we will calculate an upper bound for the second term of the RHS. We have

$$\left|\Re\left\{\int_{-\infty}^{\infty} H(f)R_W^*(f)\,\mathrm{d}f\right\}\right| \leq \left|\int_{-\infty}^{\infty} H(f)R_W^*(f)\,\mathrm{d}f\right| \tag{91}$$

$$= \left|\int_{-\infty}^{\infty} h(t)\left(h(\tau)\star\left(\mathcal{F}^{-1}\{1-\mathrm{rect}(f,W)\}\right)(\tau)\right)^*(t)\,\mathrm{d}t\right| \tag{92}$$

$$\leq \left|\int_{-\infty}^{\infty} h_{\max}\mathrm{rect}\left(t-\frac{D_s}{2},\frac{D_s}{T}\right)\times \left(h_{\max}\mathrm{rect}\left(\tau-\frac{D_s}{2},\frac{D_s}{T}\right)\star\left(\mathcal{F}^{-1}\{1-\mathrm{rect}(f,W)\}\right)(\tau)\right)^*(t)\,\mathrm{d}t\right| \tag{93}$$

$$= h_{\max}^2\left|\int_{-\infty}^{\infty} D_s\,\mathrm{sinc}(D_sf)e^{-j2\pi f\frac{D_s}{2}}\times \left(D_s\,\mathrm{sinc}(D_sf)e^{-j2\pi f\frac{D_s}{2}}\left(1-\mathrm{rect}(f,W)\right)\right)^*\mathrm{d}f\right| \tag{94}$$

$$= h_{\max}^2D_s^2\left|\int_{-\infty}^{\infty}\mathrm{sinc}^2(D_s(f))\left(1-\mathrm{rect}(f,W)\right)\,\mathrm{d}f\right| \tag{95}$$

$$= h_{\max}^2D_s^2 2\left|\int_{W}^{\infty}\mathrm{sinc}^2(D_sf)\,\mathrm{d}f\right| \tag{96}$$

$$= h_{\max}^2D_s 2\left|\int_{WD_s}^{\infty}\mathrm{sinc}^2(\nu)\,\mathrm{d}\nu\right| \tag{97}$$

For the integral in the last line we get from [14]:

$$\int_{WD_s}^{\infty}\mathrm{sinc}(\nu)^2\,\mathrm{d}\nu = \left[\frac{\cos(2\pi\nu)}{2\pi^2\nu}-\frac{1}{2\pi^2\nu}+\frac{\mathrm{Si}(2\pi\nu)}{\pi}\right]_{\nu=WD_s}^{\nu=\infty} \tag{98}$$

$$= \frac{1}{2}-\left(\frac{\cos(2\pi WD_s)}{2\pi^2WD_s}-\frac{1}{2\pi^2WD_s}+\frac{\mathrm{Si}(2\pi WD_s)}{\pi}\right) \tag{99}$$

$$\leq \frac{1}{2}+\frac{1}{2\pi^2WD_s}-\frac{\mathrm{Si}(2\pi WD_s)}{\pi}. \tag{100}$$

Since $\lim_{t\to\infty}\mathrm{Si}(t)=\frac{\pi}{2}$, we have

$$\lim_{W\to\infty}2\Re\left\{\int_{-\infty}^{\infty} H(f)R_W^*(f)\,\mathrm{d}f\right\} = 0. \tag{101}$$

and it follows from the lower-bound (90) and the upper-bound (89) that

$$\lim_{W\to\infty} \|H_{\text{eff}}\|^2 = \|H\|^2 . \tag{102}$$

Solving equation (88) for $\|R_W\|^2$, we have

$$\|R_W\|^2 = \|H_{\text{eff}}\|^2 + 2\Re\left\{\int_{-\infty}^{\infty} H(f)R_W^*(f)\,\mathrm{d}f\right\} - \|H\|^2 . \tag{103}$$

We let W go to infinity and get

$$\begin{aligned}
\lim_{W\to\infty} \|R_W\|^2 &= \lim_{W\to\infty}\left(\|H_{\text{eff}}\|^2 + 2\Re\left\{\int_{-\infty}^{\infty} H(f)R_W^*(f)\,\mathrm{d}f\right\} - \|H\|^2\right) && (104)\\
&= \|H\|^2 - 0 - \|H\|^2 && (105)\\
&= 0. && (106)
\end{aligned}$$

Since

$$\begin{aligned}
\|R_W\|^2 &= \int_{-\infty}^{\infty} |R_W(f)|^2 \,\mathrm{d}f && (107)\\
&= \int_{-\infty}^{\infty} |(1-\mathrm{rect}(f,W))\,H(f)|^2 && (108)\\
&= \int_{-\infty}^{\infty} |H(f) - H_{\text{eff}}(f)|^2 \,\mathrm{d}f && (109)\\
&= \int_{-\infty}^{\infty} |h(\tau) - h_{\text{eff}}(\tau)|^2 \,\mathrm{d}\tau && (110)
\end{aligned}$$

we have shown that for $W\to\infty$ or equivalently for $T\to 0$, $h_{\text{eff}}(\tau)$ converges to $h(\tau)$ in the $\mathcal{L}^2(\mathcal{R})$ sense.

□

Lemma 4. *Let $\mathcal{U}$ be a linear sub-space of $\mathcal{L}^2(\mathcal{R})$. Let $\hat{\mathcal{U}}$ denote the set of all functions that are the Fourier transforms of functions in $\mathcal{U}$. Then the following statement holds: The set $\{\phi_l(t)\}$ is a complete orthonormal basis for $\mathcal{U}$ if, and only if, the set $\{\Phi_l(f)\}$ is a complete orthonormal basis for $\hat{\mathcal{U}}$.*

Proof

We took this lemma from [11] and will omit giving a proof here.

□

Lemma 5. *Any function $v(t) \in \mathcal{L}^2(\mathcal{R})$ whose frequency spectrum $X(f)$ is in $\mathcal{H}_W$ can be represented by an orthonormal expansion using the set*

$$\left\{\phi_l(t) = \frac{1}{\sqrt{T}}\operatorname{sinc}\left(\frac{t-lT}{T}\right)\right\}_{l\in\mathcal{Z}}, \quad T = \frac{1}{2W}. \tag{111}$$

In the same way, it can be represented by an orthonormal expansion using any time shifted version of (111) given by

$$\left\{\phi_l(t-d) = \frac{1}{\sqrt{T}}\operatorname{sinc}\left(\frac{t-d-lT}{T}\right)\right\}_{l\in\mathcal{Z}}, \quad T = \frac{1}{2W}. \tag{112}$$

The Hilbert space spanned by both (111) and (112) we will denote by $\mathcal{H}_T$.

Proof

This lemma follows directly from Lemma 4.

□

Lemma 6. *Let $\{\phi_l(t)\}_{l\in\mathcal{Z}}$ be an ONB of $\mathcal{H}_T$ and $x(t)$ be an element of $\mathcal{H}_T$. The squared 2-norm of $x(t)$ can then be written as*

$$\|x\|^2 = \sum_{l=-\infty}^{\infty} |\langle x(\tau), \phi_l(\tau)\rangle|^2 \tag{113}$$

Proof

For a function $x(t) \in \mathcal{H}_T$ we have

$$\begin{aligned}
\|x\|^2 &= \langle u(t), u(t)\rangle && (114)\\
&= \left\langle \sum_{l=-\infty}^{\infty} \langle x(\tau), \phi_l(\tau)\rangle\, \phi_l(t), \sum_{k=-\infty}^{\infty} \langle x(\tau), \phi_k(\tau)\rangle\, \phi_k(t) \right\rangle && (115)\\
&= \sum_{l=-\infty}^{\infty}\sum_{k=-\infty}^{\infty} \langle x(\tau), \phi_l(\tau)\rangle \langle x(\tau), \phi_k(\tau)\rangle^* \langle \phi_l(t), \phi_k(t)\rangle && (116)\\
&= \sum_{l=-\infty}^{\infty} \langle x(\tau), \phi_l(\tau)\rangle \langle x(\tau), \phi_l(\tau)\rangle^* && (117)\\
&= \sum_{l=-\infty}^{\infty} |\langle x(\tau), \phi_l(\tau)\rangle|^2 . && (118)
\end{aligned}$$

□

Theorem 2. *(Parseval) The Fourier transform is a linear mapping that maps $\mathcal{L}^2(\mathcal{R})$ onto $\mathcal{L}^2(\mathcal{R})$ and preserves inner products.*

Proof

We took this theorem from [11] and will omit giving a proof here.

□

Remark 4. *From Theorem 2 it follows that we can write the squared 2-norm of $x(t) \in \mathcal{H}_T$ as*

$$
\begin{aligned}
\|x\|^2 &= \langle x(t), x(t) \rangle && (119)\\
&= \langle X(f), X(f) \rangle && (120)\\
&= \sum_{l=-\infty}^{\infty} |\langle x(t), \phi_l(t) \rangle|^2 && (121)\\
&= \sum_{l=-\infty}^{\infty} |\langle X(f), \Phi_l(f) \rangle|^2 && (122)
\end{aligned}
$$

it can thus also be calculated in frequency domain.

Lemma 7. *Let $v(t)$ be an element of $\mathcal{H}_T$. Let $\{\phi_l(t)\}_{l \in \mathcal{Z}}$ be an ONB of $\mathcal{H}_T$ as given in Lemma 5. Let $x(t)$ be the representative of $v(t)$ such that*

$$x(t) = \int_{-\infty}^{\infty} V(f) e^{j2\pi f t} \,\mathrm{d}f. \tag{123}$$

Then

$$\langle v(t), \phi_l(t) \rangle = \sqrt{T} x(lT). \tag{124}$$

Proof

We have

$$
\begin{aligned}
\langle v(t), \phi_l(t) \rangle &= \langle V(f), \Phi_l(f) \rangle && (125)\\
&= \int_{-\infty}^{\infty} V(f) \Phi_l^*(f) \,\mathrm{d}f && (126)\\
&= \int_{-\infty}^{\infty} V(f) \frac{1}{\sqrt{2W}} \mathrm{rect}(f, W)\, e^{j2\pi f l T} \,\mathrm{d}f && (127)\\
&= \frac{1}{\sqrt{2W}} \int_{-\infty}^{\infty} V(f) e^{j2\pi f l T} \,\mathrm{d}f && (128)\\
&= \frac{1}{\sqrt{2W}} x(lT) && (129)\\
&= \sqrt{T} x(lT). && (130)
\end{aligned}
$$

□

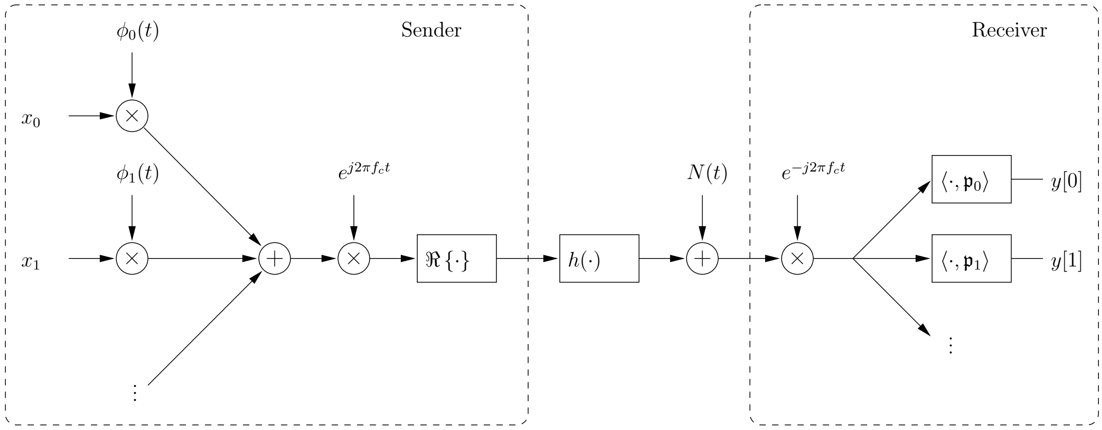

Figure 1: Digital modulation system

Remark 5. *To avoid to complicated notations, we will identify $v(t)$ with $x(t)$ whenever needed. Throughout this document, we will therefore write*

$$\langle v(t), \phi_l(t)\rangle = \sqrt{T} v(lT) \tag{131}$$

instead of (130).

C. General Discrete Time I/O Relation

In this chapter, we will derive a general discrete time I/O relation for band-limited input signals, an almost arbitrary LTI channel and additive white Gaussian noise and we will incorporate an unknown timing offset between sender and receiver. We start by considering pass-band communication; base-band comunication then follows as a special case.

C.1. System of Interest

You can find an illustration of the considered system in Figure 1.

We assume our input signals to be band-limited to $W = 1/2T$. We represent the complex envelope of the transmitted signal $x(t)$ by a sequence of complex symbols $\{x_l\}_{l\in\mathcal{Z}}$ modulated onto the complete orthonormal basis of $\mathcal{H}_T$ as given by equation (111). We assume

$$\sum_{l=-\infty}^{\infty} |x_l|^2 < \infty, \tag{132}$$

the complex envelope thus lies in $\mathcal{H}_T$.

The carrier signal is of frequency $f_c > 2W_r$ (we will define W_r below), the transmitted signal $x(t)$ is then given by

$$x(t) = \Re\left\{ \sum_{l=-\infty}^{\infty} x_l \phi_l(t) e^{j2\pi f_c t} \right\}. \tag{133}$$

We describe the channel by its frequency spectrum $H(f)$, and we assume, that it essentially takes finite values in the frequency band of interest, in our case given by $[f_c - W, f_c + W]$.

We assume to have sampling clocks without drift at the sender and the receiver. However, we introduce a timing offset in the same way as in Chapter 2. We will denote the timing offset by d. The time at the receiver t_r is thus related to the time at the sender t by $t_r = t - d$. Throughout the rest of this document, we will refer to these two time references by t and $t - d$.

At the receiver we project the down-converted received signal onto the space $\mathcal{H}_{T_r}$ with $T_r \leq T$. This corresponds to a bandwidth $W_r = 1/2T_r \geq W$; we have thus $\mathcal{H}_T \subseteq \mathcal{H}_{T_r}$ and the projection completely describes the received signal. In $\mathcal{H}_{T_r}$, we represent the signal by the orthonormal basis given by

$$\left\{\mathfrak{p}_l(t) = \frac{1}{\sqrt{T_r}} \operatorname{sinc}\left(\frac{t - lT_r}{T_r}\right)\right\}_{l \in \mathcal{Z}}, \quad T_r = \frac{1}{2W_r}. \tag{134}$$

C.2. I/O Relation for Passband Communication

As stated above, for the real signal $x(t)$ transmitted by the sender we have, in the time domain,

$$x(t) = \Re\left\{\sum_{l=-\infty}^{\infty} x_l \phi_l(t) e^{j2\pi f_c t}\right\}. \tag{135}$$

For a complex signal $v(t)$, we can write the Fourier transform of its real part as

$$\mathcal{F}\left\{\Re\left\{v(t)\right\}\right\} = \frac{V(f) + V^*(-f)}{2}, \tag{136}$$

We thus get for the signal $x(t)$ in the frequency domain

$$X(f) = \frac{1}{2}\sum_{l=-\infty}^{\infty} x_l \Phi_l(f - f_c) + \frac{1}{2}\sum_{l=-\infty}^{\infty} x_l^* \Phi_l^*(-f - f_c) \tag{137}$$

$$= \frac{1}{2}\sum_{l=-\infty}^{\infty} \left(x_l \Phi_l(f - f_c) + x_l^* \Phi_l(f + f_c)\right) \tag{138}$$

where the second line follows because $\Phi_l(f)$ is conjugate symmetric in f. The frequency spectrum $Y(f)$ of the received signal $y(t)$ is given by

$$Y(f) = X(f)H(f). \tag{139}$$

At the receiver, we process $y(t)$ taking into account the time offset d, which is in time domain equivalent to evaluating every function of time at the receiver in $t - d$. In the frequency domain, this corresponds to multiplying every function of frequency at the receiver by the phase-shift $e^{-j2\pi fd}$. The left-shift in frequency domain of the received signal $y(t)$ yields at the receiver

$$Y_B(f) = \left(Y(\nu) \star \delta(\nu + f_c) e^{-j2\pi\nu d}\right)(f) \tag{140}$$
$$= Y(f + f_c) e^{-j2\pi f_c d} \tag{141}$$
$$= X(f + f_c) H(f + f_c) e^{-j2\pi f_c d}. \tag{142}$$

We then project $y_B(t)$ onto the basis functions $\{\mathfrak{p}_k(t)\}_{k\in\mathcal{Z}}$ evaluated in $t - d$ to get $y[k]$. To make sure that the inner products are well defined, we pre-filter $Y_B(f)$ by $\mathrm{rect}(f, W)$:

$$y[k] = \left\langle Y_B(f)\mathrm{rect}(f, W), \mathfrak{P}_k(f) e^{-j2\pi fd} \right\rangle \tag{143}$$
$$= \left\langle X(f + f_c) H(f + f_c) e^{-j2\pi f_c d} \mathrm{rect}(f, W), \mathfrak{P}_k(f) e^{-j2\pi fd} \right\rangle \tag{144}$$
$$= \left\langle \frac{1}{2} \sum_{l=-\infty}^{\infty} \left(x_l \Phi_l(f) + x_l^* \Phi_l(f + 2f_c)\right) H(f + f_c) e^{-j2\pi f_c d} \mathrm{rect}(f, W), \mathfrak{P}_k(f) e^{-j2\pi fd} \right\rangle \tag{145}$$
$$= \left\langle \frac{1}{2} \sum_{l=-\infty}^{\infty} x_l \Phi_l(f) H(f + f_c) e^{-j2\pi f_c d}, \mathfrak{P}_k(f) e^{-j2\pi fd} \right\rangle \tag{146}$$
$$= \frac{1}{2} \sum_{l=-\infty}^{\infty} x_l e^{-j2\pi f_c d} \left\langle \sqrt{T} \mathrm{rect}(f, W)\, e^{-j2\pi f l T} H(f + f_c), \mathfrak{P}_k(f) e^{-j2\pi fd} \right\rangle \tag{147}$$
$$= \frac{\sqrt{T}}{2} \sum_{l=-\infty}^{\infty} x_l e^{-j2\pi f_c d} \left\langle H(f + f_c)\mathrm{rect}(f, W), \mathfrak{P}_k(f) e^{-j2\pi f(d - lT)} \right\rangle \tag{148}$$

The term $H(f + f_c)\mathrm{rect}(f, W)$ is the low-pass filtered frequency spectrum of the channel in the base-band. We define it as the frequency spectrum of the effective channel:

$$H_{\mathrm{eff}}(f) = H(f + f_c)\mathrm{rect}(f, W). \tag{149}$$

For $y[k]$ we further get

$$y[k] = \frac{\sqrt{T}}{2} \sum_{l=-\infty}^{\infty} x_l e^{-j2\pi f_c d} \left\langle H_{\text{eff}}(f), \mathfrak{P}_k(f) e^{-j2\pi f(d-lT)} \right\rangle \tag{150}$$

$$= \frac{\sqrt{T}}{2} \sum_{l=-\infty}^{\infty} x_l e^{-j2\pi f_c d} \left\langle H_{\text{eff}}(f), \sqrt{T_r}\text{rect}(f, W_r)\, e^{-j2\pi f k T_r} e^{-j2\pi f(d-lT)} \right\rangle \tag{151}$$

$$= \frac{\sqrt{T}}{2} \sum_{l=-\infty}^{\infty} x_l e^{-j2\pi f_c d} \int_{-\infty}^{\infty} H_{\text{eff}}(f) \sqrt{T_r}\text{rect}(f, W_r)\, e^{j2\pi f k T_r} e^{j2\pi f(d-lT)}\, \mathrm{d}f \tag{152}$$

$$= \frac{\sqrt{TT_r}}{2} \sum_{l=-\infty}^{\infty} x_l e^{-j2\pi f_c d} \int_{-\infty}^{\infty} H_{\text{eff}}(f) e^{j2\pi f(kT_r - lT + d)}\, \mathrm{d}f \tag{153}$$

$$= \frac{\sqrt{TT_r}}{2} \sum_{l=-\infty}^{\infty} x_l h_{\text{eff}}(kT_r - lT + d) e^{-j2\pi f_c d}, \tag{154}$$

where we used the property of the basis given by Lemma 7.

C.3. Additive White Gaussian Noise

In the following, we calculate the effects of the processing at the receiver onto the additive noise $N(t)$. We assume $N(t)$ to be zero mean white Gaussian noise of power N_0 over the frequency of interest. At every time instant, $N(t)$ is distributed according to $\mathcal{N}(0, N_0)$ and the autocorrelation of $N(t)$ is given by

$$\mathbb{E}[N(t)N^*(\tau)] = \delta(t - \tau)N_0. \tag{155}$$

Since $N(t) \notin \mathcal{L}^2(\mathcal{R})$ according to our assumption, we avoid the notation of inner products. For the projection of $N(t)e^{-j2\pi f_c d}$ onto the basis functions evaluated in $t - d$ we formally have for the coefficients:

$$N[k] = \int_{-\infty}^{\infty} N(t) e^{-j2\pi f_c (t-d)} \mathfrak{p}_l^*(t - d)\, \mathrm{d}t. \tag{156}$$

these integrals might not convert for certain realizations of $N(t)$, however, we see that these integrals describe linear functionals of $N(t)$. They are thus Gaussian themselves. We can completely characterize them by the mean, covariance and pseudo-covariance, see [15]. For the mean we get

$$\mathbb{E}[N[k]] = \mathbb{E}\left[\int_{-\infty}^{\infty} N(t)\mathfrak{p}_l^*(t - d) e^{-j2\pi f_c (t-d)}\, \mathrm{d}t\right] \tag{157}$$

$$= \int_{-\infty}^{\infty} \mathbb{E}[N(t)]\, \mathfrak{p}_l^*(t - d) e^{-j2\pi f_c (t-d)}\, \mathrm{d}t \tag{158}$$

$$= 0. \tag{159}$$

For the covariance we get

$$\mathbb{E}[N[l]N^*[k]] = \mathbb{E}\left[\left(\int_{-\infty}^{\infty} N(t)\mathfrak{p}_l^*(t-d)e^{-j2\pi f_c(t-d)}\,\mathrm{d}t\right) \times \left(\int_{-\infty}^{\infty} N(\tau)\mathfrak{p}_k^*(\tau-d)e^{-j2\pi f_c(\tau-d)}\,\mathrm{d}\tau\right)^*\right] \tag{160}$$

$$= \mathbb{E}\left[\int_{-\infty}^{\infty}\int_{-\infty}^{\infty} N(t)\mathfrak{p}_l^*(t-d)e^{-j2\pi f_c(t-d)} \times N^*(\tau)\mathfrak{p}_k(\tau-d)e^{j2\pi f_c(\tau-d)}\,\mathrm{d}t\,\mathrm{d}\tau\right] \tag{161}$$

$$= \int_{-\infty}^{\infty}\int_{-\infty}^{\infty} \mathbb{E}[N(t)N^*(\tau)]\,\mathfrak{p}_l^*(t-d)\mathfrak{p}_k(\tau-d)\,\mathrm{d}t\,\mathrm{d}\tau \tag{162}$$

$$= \int_{-\infty}^{\infty}\int_{-\infty}^{\infty} \delta(t-\tau)N_0\mathfrak{p}_l^*(t-d)\mathfrak{p}_k(\tau-d)\,\mathrm{d}t\,\mathrm{d}\tau \tag{163}$$

$$\overset{(a)}{=} \mathbf{N_0}\int_{-\infty}^{\infty} \mathfrak{p}_l^*(t-d)\mathfrak{p}_k(t-d)\,\mathrm{d}t \tag{164}$$

$$= \mathbf{N_0}\delta[l-k], \tag{165}$$

where (a) results from

$$\int_{-\infty}^{\infty} N_0\delta(t)\,\mathrm{d}t = \mathbf{N_0}. \tag{166}$$

The symbol N_0 represents power of noise and $\mathbf{N_0}$ represents energy of noise; it is the result of integrating N_0 multiplied with the dimensionless distribution $\delta(t)$ over time.

For the pseudo-covariance we get

$$\begin{aligned}\mathbb{E}[N[l]N[k]] &= \mathbb{E}\Bigg[\int_{-\infty}^{\infty}\int_{-\infty}^{\infty} N(t)\mathfrak{p}_l^*(t-d)e^{-j2\pi f_c(t-d)} \times \\ &\qquad N(\tau)\mathfrak{p}_k^*(\tau-d)e^{-j2\pi f_c(\tau-d)}\,\mathrm{d}t\,\mathrm{d}\tau\Bigg] \qquad (167)\\ &= \int_{-\infty}^{\infty}\int_{-\infty}^{\infty} \mathbb{E}[N(t)N(\tau)]\,\mathfrak{p}_l^*(t-d)\mathfrak{p}_k^*(\tau-d)e^{-j2\pi f_c(t+\tau-2d)}\,\mathrm{d}t\,\mathrm{d}\tau \qquad (168)\\ &= \int_{-\infty}^{\infty}\int_{-\infty}^{\infty} \delta(t-\tau)N_0\mathfrak{p}_l^*(t-d)\mathfrak{p}_k^*(\tau-d)e^{-j2\pi f_c(t+\tau-2d)}\,\mathrm{d}t\,\mathrm{d}\tau \qquad (169)\\ &= \mathbf{N_0}\int_{-\infty}^{\infty} \mathfrak{p}_l^*(t-d)\mathfrak{p}_k^*(t-d)e^{-j4\pi f_c(t-d)}\,\mathrm{d}t \qquad (170)\\ &= \mathbf{N_0}\int_{-\infty}^{\infty} \mathfrak{p}_l^*(t)\mathfrak{p}_k^*(t)e^{-j4\pi f_c t}\,\mathrm{d}t \qquad (171)\\ &\overset{(a)}{=} \mathbf{N_0}\int_{-\infty}^{\infty} \mathfrak{P}_l^*(-f)\mathfrak{P}_k^*(-f-2f_c)\,\mathrm{d}f \qquad (172)\\ &= 0, \qquad (173)\end{aligned}$$

where (a) follows because the basis functions are band-limited to W_r and $f_c > 2W_r$. Since the covariance vanishes for $l \neq k$ and since the pseudo-covariance vanishes everywhere, $N[k]$ are i.i.d. circular symmetric complex Gaussian distributed according to $\mathcal{CN}(0, \mathbf{N_0})$.

C.4. The Complete I/O Relation

Adding the noise term, the complete I/O relation for the pass-band is given by

$$y[k] = \frac{\sqrt{TT_r}}{2}\sum_{l=-\infty}^{\infty} x_l h_{\text{eff}}(kT_r - lT + d)e^{-j2\pi f_c d} + N[k], \quad N[k] \sim \mathcal{CN}(0, \mathbf{N_0}). \qquad (174)$$

We can obtain the I/O relation for the base-band case by assuming the input sequence $\{x_l\}_{l\in\mathcal{Z}}$ to take on real values only and setting the carrier frequency f_c to zero. The derivation then follows the same lines as in the pass-band case; here we will only give the result which is

$$y[k] = \sqrt{TT_r}\sum_{l=-\infty}^{\infty} x_l h_{\text{eff}}(kT_r - lT + d) + N[k], \quad N[k] \sim \mathcal{N}(0, \mathbf{N_0}). \qquad (175)$$

The differences to the pass-band case are the missing factor 1/2, the missing phase-shift $e^{-j2\pi f_c d}$ and the different frequency spectrum of the effective channel. In the pass-band case, it is given by

$$H_{\text{eff}}(f) = H(f + f_c)\text{rect}(f, W) \tag{176}$$

and the effective impulse response $h_{\text{eff}}(\tau)$ is complex valued whereas in the base-band case it is given by

$$H_{\text{eff}}(f) = H(f)\text{rect}(l, W)\,. \tag{177}$$

with the effective impulse response $h_{\text{eff}}(\tau)$ being real valued. In addition, the discrete time noise $N[k]$ is in the pass-band case i.i.d. circular symmetric complex Gaussian whereas it is i.i.d. real Gaussian in the base-band case.

C.5. Physical Units

We interpret the signal $x(t) \in \mathcal{H}_T$ as a voltage changing over time. With the following units, the derivations in this paper are consistent with the physical reality:

$[T] = \text{s}$	$[W] = \text{Hz}$	$[\|x\|^2] = \text{J}\Omega$	$[x(t)] = \text{V}$
$[X(f)] = \frac{\text{V}}{\text{Hz}}$	$[h(\tau)] = \text{Hz}$	$[H(f)] = 1$	

Table 1: Physical units for the derivations in this chapter.

D. Band-limited Signals in Time Domain

The most important theorem in digital communications is probably the Sampling Theorem. In any introductory course in communication, the students are exposed to this theorem. Two excellent handouts introducing the signal-space concept and the Sampling Theorem are [5] and [16]; both written by R. G. Gallager. During this chapter, we assume that you are familiar to the concepts introduced in these two handouts.

The Sampling Theorem states that if a signal $x(t)$ is band limited to W, then it can be represented exactly by its samples if they are taken at integer multiples of $T = 1/2W$. Probably for reasons of simple notation, it is convenient to choose the set $\{x(lT)\}_{l\in\mathcal{Z}}$ to represent $x(t)$ by its samples. However, we can represent $x(t)$ by *any* set of the form $\{x(lT)\}_{l\in\mathcal{Z}}$ where $d \in \mathcal{R}$ is arbitrary but constant. We state this property in Lemma 5 in Appendix B. In this chapter, however, we want to stress your intuition.

During our studies, we learned to switch to the frequency domain whenever applying a low-pass filter to a signal: it is much easier to perform multiplication in frequency domain than it is to perform convolution in time domain. However, as a side-effect, we never trained our intuition about what actually happens in time domain when passing a signal through a low-pass filter. We will therefor focus on the time domain in this chapter. To illustrate the discussion, we choose an analog which is more accessible to the human imagination then electromagnetic waveforms: we represent the signal by an image of a sequence of letters printed to a paper. Low-pass filtering the signal we will perform by convolving the image with a 2D-sinc function and sampling we represent by values the image takes in lattice points.

Figure 2: Original image.

Figure 3: Image filtered by a 2D-sinc function corresponding to a sampling width of $T = 12$ pixels.

It is often stated that a low-pass filtered signal is globally spread in time. While the unfiltered signal might be finite in time, the filtered signal is not- it takes nonzero values over the whole axis of real numbers. Theoretically, this is a fundamental problem and practically, it is not. A nice discussion of this dilemma you can find in the article [10] of David Slepian.

Much more relevant in practice is that a low-pass filtered signal is also locally spread in time. The low-pass filtered version of our signal $x(t)$ is given by

$$y(t) = \int_{-\infty}^{\infty} x(t-\tau)h(\tau)\,\mathrm{d}\tau. \tag{178}$$

where h is given by

$$h(\tau) = \frac{1}{T}\,\mathrm{sinc}\left(\frac{\tau}{T}\right). \tag{179}$$

When we take a closer look at the convolution integral we can see that at every time instant t_0, $y(t_0)$ contains information about *all* values that $x(t)$ takes over the real axis. However, the influence of $x(t)$ onto $y(t_0)$ decreases when the distance between t and t_0 gets large. Looking at a plot of the sinc function we can say that the values $x(t)$ takes in $[t_0 - T/2, t_0 + T/2]$ have the greatest influence on the value of $y(t_0)$.

Figure 4: The original image was scaled down by a factor of 2 and then filtered by the sinc function with parameter $T = 12$ pixels.

Although all values that $x(t)$ takes over the real axis have influence onto $y(t)$, we can only recover a part of the information contained in $x(t)$ from $y(t)$. To explain this, we interpret the convolution with the sinc as a blur-filter. It smooths out local variation. What locality means is stated by the Sampling Theorem: we can recover the filtered signal from its samples taken equally spaced by T, so in an interval of length T there is not more information then the information contained in one sample. This interpretation can be related to the notion of degrees of freedom of a low-pass filtered signal: it states that a signal of bandwidth W has over a duration of D roughly $2WD$ degrees of freedom. But since $T = 1/2W$, we have $2WD = D/T$ and this is simply the number of samples we take in D. Shannon introduced this notion of degrees of freedom in [17]; it was Slepian who mathematically proved its asymptotic correctness. You can find a proof in [10].

Looking at figure 2, we choose a naive heuristics to determine what locality is in this context: we look for the smallest thickness T of the letters. We find $T = 12$ pixels and say that a square of side-length T is a local area. When we filter the image by a 2D-sinc function with parameter $T = 12$ we get figure 3; as we can see, the information is preserved, we can still read the letters. If we first scale the figure by a factor of 0.5 and then filter it with the same 2D-sinc function, we end up with figure 4. In this case, the information is not preserved, we can no longer read the letters. We can explain this in the following way: since we scaled by a factor of 0.5, the image now variates locally every 6 pixels. However, we filtered it by a 2D sinc function with parameter $T = 12$ pixels and thus smoothed out local variations over distances shorter then 12 pixels.

Since we low-pass filtered our signal, we can apply the Sampling Theorem and represent it by its samples obtained by evaluating the filtered image in lattice points of a lattice with a lattice size of $T = 12$ pixels. As argued above, the information is mainly spread locally so we use a lattice a bit larger then the letter sequence. The origin of the lattice in the upper left corner we let our octave script randomly choose in a square of side length $T = 12$ pixels. Since the lattice is periodic with T both in vertical and horizontal direction we can say that we choose an arbitrary lattice. Two possible sample sets you find in the figures 5 and 6.

For the human eye, it is difficult to interpolate the sample points and identify the

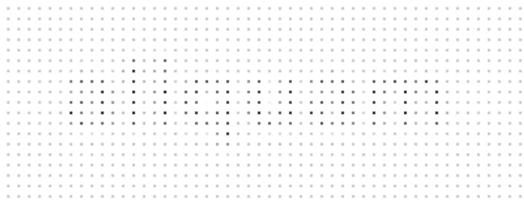

Figure 5: First sample-set of the filtered image with lattice size $T = 12$ pixels and lattice origin in $(63, 56)$.

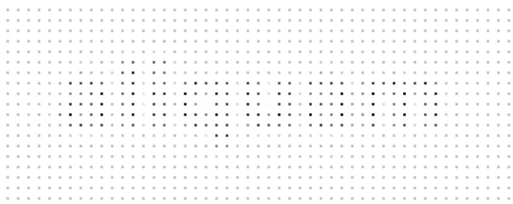

Figure 6: Second sample-set of the filtered image with lattice size $T = 12$ pixel and lattice origin in $(63, 60)$.

Figure 7: The result of interpolating the first sample-set of the filtered image with the 2D-sinc function.

letters. When we interpolate the samples by the 2D-sinc function with parameter $T = 12$ pixels, we get the figures 7 and 8. Although the origins of the lattices differ, we can in both cases read the letters; sampling thus preserved the information as predicted by the Sampling Theorem.

When we sample and interpolate the filtered version of the scaled image we end up with figure 9. Not surprisingly, we cannot read the letters, the information has got lost.

In both cases, we represented the images with the same number of samples. However, the number of samples we took in the region of interest differ, since we used the same lattice size for the large and the small picture. This illustrates that the main part of the information stays local when low-pass filtering a signal- the most part of the samples we considered in the case of the small picture did not contain much information of interest and we thus could not reconstruct the letters in a readable way. As stated above, this stands in contrast to the fact that the filtered signal is theoretically spread over the whole real axis (or in our case, the whole 2 dimensional real plane).

On the other hand, the information is locally spread. In the case of the large image we could reconstruct the letters independent from the randomly chosen origin of the lattice. This can be related to the notion of degrees of freedom: if the information contained in our sample sets would depend on the origin we choose for our lattice, then we would at least have 2 more degrees of freedom because we could choose the vertical and horizontal coordinate of the origin independent from each other.

To say it in a different way, if the information contained in the lattice points would depend on the origin of the lattice, then the filtered image would have significant variations over distances less then T. But as we have seen in the case of the small image, these variations are completely smoothed out when convolving the image with a 2d-sinc function.

Looking at figure 3 we percept that filtering the original image led to a loss of resolution—we can no longer determine where exactly the letters start and where they end. Starting in a black point in the top part of the letter a we can say "the letter a is here" and going up $T = 12$ pixels we can say "the letter a is not here". In between, we cannot say if the letter a is there or not. We introduce the notion of uncertainty and say that in a signal low-pass filtered by W, information can only be localized with a uncertainty of $T = 1/2W$.

Figure 8: The result of interpolating the second sample-set of the filtered image with the 2D-sinc function.

Figure 9: The original image was scaled down by a factor of 2 and then filtered by the sinc function with parameter $T = 12$ pixels.

In summary, we can say that passing a signal through a low-pass filter of bandwidth W has the following effects in time domain:

- Local variations over intervals smaller then $T = 1/2W$ are smoothed out.
- Although the signal is spread over the whole real axis, the main part of the information stays local.
- The degrees of freedom of a filtered signal is roughly limited to the number of samples.
- We can localize information with an uncertainty of about T.

References

[1] D. N. C. Tse and P. Viswanath, *Fundamentals of Wireless Communications*, Cambridge, U.K., 2005.

[2] I. E. Telatar and D. N. C. Tse, "Capacity and mutual information of wideband multipath fading channels," *IEEE Trans. Inf. Theory*, vol. 46, no. 4, pp. 1384–1400, Jul. 2000.

[3] M. Z. Win and R. A. Scholtz, "Characterization of ultra-wide bandwidth wireless indoor channels: A communication-theoretic view," *IEEE J. Sel. Areas Commun.*, vol. 20, no. 9, pp. 1613–1627, Dec. 2002.

[4] U. G. Schuster and H. Bölcskei, "Ultra-wideband channel modeling on the basis of information-theoretic criteria," *IEEE J. Sel. Areas Commun.*, 2005, submitted.

[5] R. G. Gallager, "Signal space concepts," lecture Notes. [Online]. Available: http://www.nari.ee.ethz.ch/commth/teaching/wirelessIT/handouts/signal_space.pdf

[6] "Channel (communications)," Wikipedia, accessed 01.07.06. [Online]. Available: http://en.wikipedia.org/wiki/Communications_channel

[7] P.-G. Fontolliet, *Système de Télécommunications*, ser. Traité d'Électricité. Presses polytechniques et universitaires romndes, 1999, vol. XVIII.

[8] S. Haykin, *Communication Systems*, 4th ed. John Wiley & Sons, 2001.

[9] H. Meyr, M. Moeneclaey, and S. A. Fechtel, *Digital Communication Receivers*, New York, NY, 1998.

[10] D. Slepian, "On bandwidth," in *Proc. IEEE*, vol. 64, no. 3, mar 1976.

[11] A. Lapidoth, "Information transfer," Jul. 2005, lecture Notes for the course "Information Transfer", ETHZ.

[12] U. Lang, “Mass und integral,” 2005, lecture Notes for the course “Mass und Integral”, ETHZ. [Online]. Available: http://www.math.ethz.ch/~gruppe5/group5/lectures/masstheorie/ss06/masstheorie-ss05.pdf

[13] M. Sugiura, *Unitary Representations and Harmonic Analysis.* John Wiley & Sons, 1975.

[14] A. W. W. Resource, “The integrator,” http://integrals.wolfram.com, Since 1996.

[15] I. E. Telatar, “Mathematical preliminaries,” Mar. 2003, handout for the course “Wireless Communications and Mobility”, EPFL. [Online]. Available: http://lthiwww.epfl.ch/WCM/ln2.pdf

[16] R. G. Gallager, “The sampling theorem,” lecture Notes. [Online]. Available: http://www.nari.ee.ethz.ch/commth/teaching/wirelessIT/handouts/sampling.pdf

[17] C. E. Shannon, “A mathematical theory of communication,” vol. 27, pp. 379–423 and 623–656, July and October 1948.